ARTICLE IN PRESS

Available online at www.sciencedirect.com

SCIENCE DIRECT

ELSEVIER

Planetary and Space Science ▮ (▮▮▮▮) ▮▮▮–▮▮▮

Planetary and Space Science

www.elsevier.com/locate/pss

Galileo long-term dust monitoring in the jovian magnetosphere

Harald Krüger[a,b,*], Gudrun Linkert[b], Dietmar Linkert[b], Richard Moissl[b], Eberhard Grün[b,c]

[a] *Max-Planck-Institut für Sonnensystemforschung, Max-Planck-Str. 2, 37191 Katlenburg-Lindau, Germany*

[b] *Max-Planck-Institut für Kernphysik, Postfach 10 39 80, 69029 Heidelberg, Germany*

[c] *Hawaii Institute of Geophysics and Planetology, University of Hawaii, 1680 East West Road, Honolulu, HI 96822, USA*

Received 22 March 2004; received in revised form 18 April 2005; accepted 20 April 2005

Abstract

The Galileo spacecraft was launched in 1989, and—between 1995 and 2003—was the first spacecraft in orbit about Jupiter. The in-situ dust instrument on board was a highly sensitive impact-ionisation dust detector which measured the speed, mass and impact direction of dust particles hitting a metal target. It provided a unique 12-year record of cosmic dust in interplanetary and circumjovian space. Degradation of the instrument electronics caused by the harsh radiation environment in the inner jovian magnetosphere was recognised in various ways: the sensitivity for dust detection dropped by a factor of 7.5 between 1996 and 2003 while the noise sensitivity decreased by up to a factor of 100. Shifts in the parameters measured during dust impacts and noise events (charge amplitudes and signal rise times, etc.) required a time-dependent algorithm for noise identification. After noise removal a total of 21 224 complete data sets for dust impacts (i.e. impact charges, signal rise times, impact direction, etc.) is available from the entire Galileo mission between 1989 and 2003 (18 340 data sets from the Jupiter mission after 1996). This homogeneous data set has been used in many investigations of jovian dust published already or ongoing. Electronics degradation prevents the application of the mass and speed calibration to data obtained after 2000. Only in cases where the impact speed of grains is known by other means can grain masses be derived for later measurements. The drop of the detection sensitivity also required a time-dependent correction for fluxes of jovian dust streams, reaching a factor of 20 in 2002. We use the derived homogeneous noise-removed data set for long-term monitoring of the jovian dust streams with Galileo. The derived fluxes of dust stream particles were highly variable by about five orders of magnitude, between 3×10^{-3} and $6 \times 10^{2}\,\mathrm{m^{-2}\,s^{-1}}$ and exhibited strong orbit-to-orbit variability. This extensive and valuable data set is available for further detailed investigations.

Keywords: Dust; Space instrumentation

1. Introduction

The Galileo spacecraft was launched in 1989, and between 1995 and 2003 it was the first Jupiter-orbiting spacecraft, completing 34 revolutions about the planet. The dust instrument on board was a highly sensitive impact ionisation dust detector (Grün et al., 1992), more sensitive than any other space-born in-situ dust instrument flown before. Many new phenomena were successfully explored with the dust instrument in the fields of interplanetary, interstellar and circumplanetary dust research.

The dust sensor was in continuous operation during the entire Galileo mission (Grün et al., 1995b; Krüger et al., 1999a, 2001) and provided long-term in-situ dust measurements in the environment of Jupiter for the first time. A wealth of dust phenomena was investigated in-situ (see also Grün et al., 2001; Krüger, 2003, for recent reviews): jovian dust streams originating from Jupiter's moon Io (Morfill et al., 1980; Horányi et al., 1997; Grün

*Corresponding author. Max-Planck-Institut für Sonnensystemforschung, Max-Planck-Str. 2, 37191 Katlenburg-Lindau, Germany.

E-mail address: krueger@linmpi.mpg.de (H. Krüger).

0032-0633/$ - see front matter © 2005 Elsevier Ltd. All rights reserved.
doi:10.1016/j.pss.2005.04.009

et al., 1998; Graps et al., 2000, Krüger et al., 2003a,b), impact-generated dust clouds surrounding the Galilean moons (Krüger et al., 1999c, 2000, 2003c; Sremčević et al., 2005), a tenuous dust ring in the region between the Galilean moons (Thiessenhusen et al., 2000; Krivov et al., 2002a) and further out from the moons (Krivov et al., 2002b), as well as interplanetary and interstellar particles captured by the jovian magnetosphere (Colwell et al., 1998a,b). Most of these studies relied on a data set collected over many years in order to derive statistically meaningful results because dust impact rates are usually very low. Hence, stable instrument operation over the years was a prerequisite for these studies.

During its orbital mission about Jupiter the spacecraft was exposed to the harsh radiation environment of the planet's inner magnetosphere and it was anticipated that the high radiation dose acquired during 34 revolutions would cause damage in the spacecraft electronics and the scientific instruments on board. Although numerous radiation-related degradation effects were recognised, no severe failure occurred. For the dust instrument several degradation effects were revealed in the data. The most severe changes were a drop in the detection sensitivity of the instrument, and changes in the noise response and in the mass and speed calibration.

The aim of this paper is twofold. We first analyse the instrument degradation caused by the high-radiation environment of the inner jovian magnetosphere and derive quantitative corrections where possible. This leads to a homogeneous dust data set corrected for instrument degradation. This data set has already been used for many of the investigations cited above. A detailed explanation of these corrections, however, has not yet been published. We then use the corrected data set from the entire Galileo Jupiter mission for monitoring of the jovian dust streams originating from Io.

After a description of the Galileo dust instrument in Section 2, we analyse its long-term stability for dust impact detection in Section 3. Section 4 deals with countermeasures for instrument operation and data processing to counterbalance the instrument degradation and to obtain a homogeneous dust data set. Its value is illustrated by long-term monitoring of the jovian dust streams in Section 5.

2. Dust impact detection

The Galileo dust instrument has been described in detail in earlier publications (Grün et al., 1992, 2001; Krüger, 2003) and only the most important aspects are repeated here. Dust particles hitting a gold-covered metal target vaporise, and the resulting plasma cloud is detected by up to three independent charge signals (Fig. 1): The negative electron charge, Q_E, is measured on the sensor target, positive ions are accelerated towards an ion collector by an electric field and measured as a positive charge signal, Q_I. A fraction of the ions reaching the ion collector passes through the collector and is measured by a channeltron, Q_C. The charge amplitudes, Q_E and Q_I, and corresponding signal rise times, t_E and t_I, are used for mass and speed calibration: First, the impact speed v of a particle is derived from the rise times of the two charge signals. Once the speed is known, the mass m of the particle is derived from the two charge amplitudes.

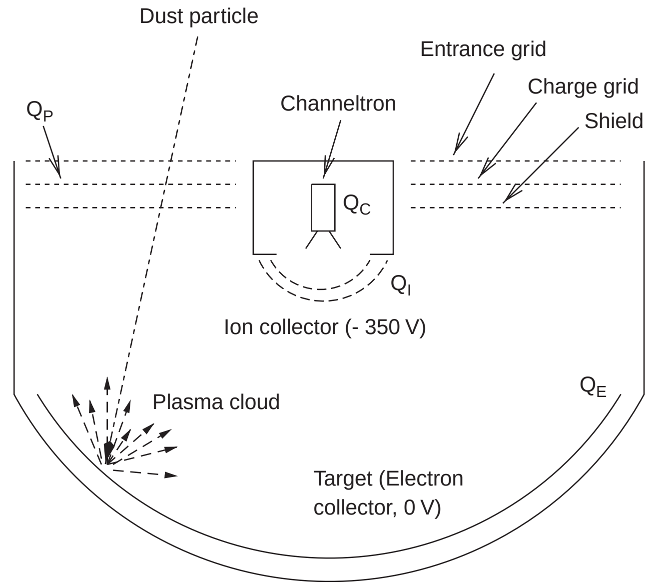

Fig. 1. Schematic configuration of the Galileo dust detector. Particles hitting the target create a plasma cloud and up to three charge signals (Q_I, Q_E, Q_C) are used for dust impact identification.

The total amount of charge, Q, collected on each channel is a function of mass m and speed v of the particle as well as the particle's composition. Q can be described by the empirical law

$$Q \propto m^{\alpha} v^{\beta}, \tag{1}$$

with $\alpha \approx 1$ and $1.5 \lesssim \beta \lesssim 5.5$ in the speed range $2 \lesssim v \lesssim 80\,\mathrm{km\,s^{-1}}$ (Auer, 2001). In particular, for constant impact speed, the charge generated upon impact is proportional to the particle mass (Göller and Grün, 1985). The calibrated speed range of the dust instrument is 2–$70\,\mathrm{km\,s^{-1}}$ for particles in the mass range $10^{-18}\,\mathrm{kg} \leqslant m \leqslant 10^{-13}\,\mathrm{kg}$. The uncertainty in the speed calibration is typically a factor of two, and consequently the mass can only be determined with a factor of ten accuracy.

The coincidence times of the three charge signals together with the charges themselves are used to classify each impact into one of four categories. Class 3 impacts have three charge signals, two are required for class 2 and class 1 events, and only one for class 0 (Baguhl, 1993; Grün et al., 1995a; Krüger et al., 1999a). Class 3, our highest quality class, contains real dust impacts and class 0 contains noise events. Class 1 and class 2 events were true dust impacts in interplanetary space (Baguhl et al., 1993; Krüger et al., 1999a). In the jovian system, within about 15 R_J distance from Jupiter (Jupiter radius, $R_J = 71492$ km), energetic particles from the jovian plasma environment caused an enhanced noise rate in class 2 and the lower quality classes. By analysing the properties of the Io stream particles and comparing them with the noise events, the noise could be eliminated from the class 2 data from the early Galileo mission (Krüger et al., 1999b). All class 0 and class 1 events detected in the jovian environment are usually classified as noise.

Each measured signal (noise event or dust impact) is classified according to the strength of its ion charge signal into one of six amplitude ranges (AR1–AR6), leading to a total of 24 different categories (4 classes times 6 amplitude ranges). Each amplitude range corresponds to about one decade in charge Q_I. The dust instrument was equipped with 24 accumulators which counted impacts in each of the 24 categories. A complete history of dust impacts can be derived this way.

Galileo was a dual-spinning spacecraft with an antenna (negative spin axis direction) usually pointing toward Earth. The dust detector (Fig. 1) was mounted on the spinning section of the spacecraft with the sensor axis being offset by 60° from the positive spin axis (i.e. usually the anti-Earth direction; Krüger et al., 1999b). The field of view of the dust detector was a cone of 140° full angle. The sensor area for impacts was a function of the angle between the impact direction and the spin axis. The maximum sensitive area of the detector averaged over one spacecraft revolution was 235 cm^2 (Krüger et al., 1999b). The impact direction of a dust particle was determined from the spin position of the spacecraft around its spin axis at the time of impact.

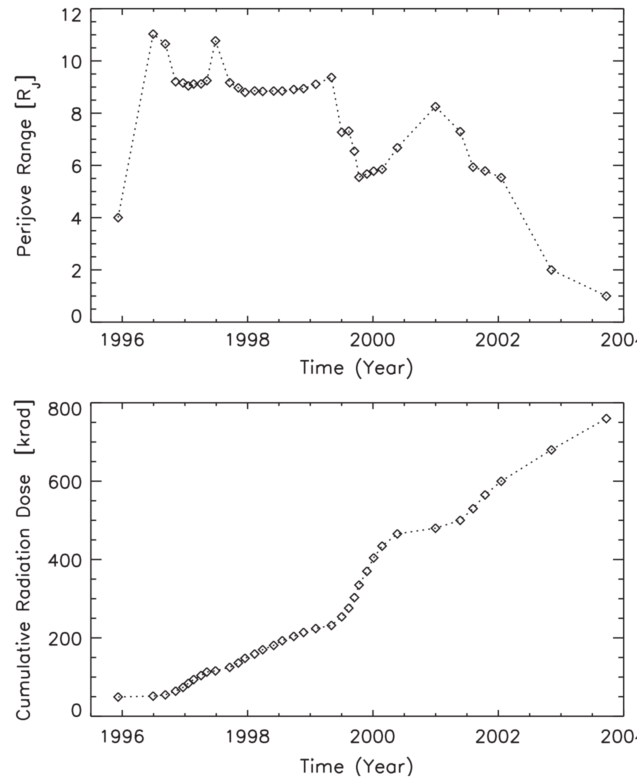

Fig. 2. Galileo perijove range (upper panel) and estimated cumulative radiation dose (bottom panel) between arrival at Jupiter in 1995 and Jupiter impact 2003 (from D. L. Bindschadler, priv. comm.).

3. Long-term operational stability of the dust instrument

During each of its 34 revolutions about Jupiter, the Galileo spacecraft was exposed to the harsh radiation environment of the inner jovian magnetosphere where energetic electrons and ions exist with energies up to several MeV and up to about 100 MeV, respectively. The spacecraft and its scientific instruments were designed to survive a radiation dose of about 123 krad until the end of Galileo's prime Jupiter mission in 1997 (O'Neil, 1997). The mission, however, was extended a few times so that the spacecraft was exposed to a total dose several times higher. Fig. 2 shows the perijove distance of Galileo's orbit about Jupiter and the total radiation dose accumulated with time. Closer to the planet the spacecraft collected a higher dose so that lower perijove distances caused a higher radiation dose per orbit (Fig. 2).

Throughout this paper we use the measured analogue values (charges, signal rise times, etc.) in physical units and the corresponding digital units (dn) in parallel. In some cases (e.g. for noise elimination) corrections are most easily and most directly applied to the 'raw' digital units rather than the physical values. Table 3 defines the digital parameters. A comprehensive description of the parameters has been given by Grün et al. (1995a).

3.1. *Instrument parameters derived from test pulses*

In order to monitor the long-term stability and to reveal changes of the instrument response to dust impacts with time, the instrument was equipped with a test pulse generator which simulated electronic signals similar to those generated by real dust impacts. These test pulses provided a means of monitoring the long-term response of the instrument to well-defined artificial "dust impacts". The instrument had three charge amplifier channels which covered six orders of magnitude in impact charge (corresponding to the six amplitude ranges, ARs, defined in Section 2). Each of the three channels had a dynamic range of two orders of magnitude. Test pulses were generated in amplitude ranges AR2, AR3 and AR5 (Table 1).

Table 1
Characteristics of the test pulse generators of the Galileo dust instrument: amplifier channel, corresponding ion charge amplitude ranges (AR) and ion charge amplitude range in which the test pulse generator created test pulses

Amplifier channel	AR	Test pulse AR
1	1,2	2
2	3,4	3
3	5,6	5

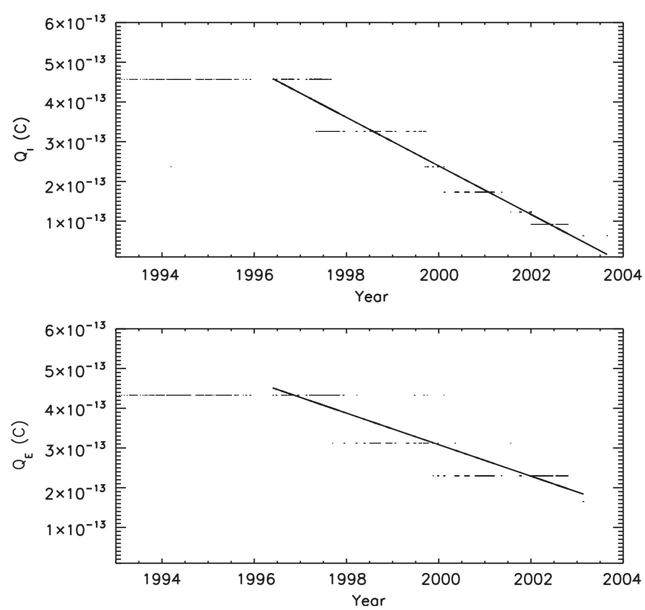

Fig. 3. Charge amplitudes Q_I and Q_E measured during the test pulses in amplitude range AR2. The horizontal steps are caused by the digitisation. Thick solid lines are linear fits to the data ($Q_I = 1.223 \times 10^{-10} - 6.103 \times 10^{-14} t$ and $Q_E = 7.966 \times 10^{-11} - 3.968 \times 10^{-14} t$; the time t is measured in years) and are used to derive Eqs. (2) and (3).

During the interplanetary cruise of Galileo, the instrument response to the test pulses remained close to the nominal values measured before launch. First changes occurred after orbit injection of the spacecraft into the Jupiter system in December 1995, i.e. after its first exposure to the high radiation levels in the jovian system: Signal rise times, charge amplitudes, time differences between charge signals and signal coincidences as measured during the test pulses shifted since then. Examples of the changes in the instrument response are shown in Fig. 3.

In the lowest channel, AR2, the charge amplitudes measured on the iongrid, IA, dropped by 6 dn which corresponds to a reduction in amplification by about a factor of 7.5. On the target channel, EA, the drop is 3 dn. The signal rise times ET and IT in AR2 have both shifted by 2 dn since launch (not shown here). Similar shifts in the rise times and amplitudes were also recognised for the test pulses in the higher channels. The shifts in AR5 were comparable to those in AR2 while those in AR3 were even larger.

The reason for these changes in the electronics' response is most likely degradation of the instrument electronics. The shifts in the test pulses began in 1996 after Galileo was first exposed to the high radiation of the jovian magnetosphere. The three channels IA, CA and EA use the same type of operational amplifier whereas the PA channel is connected to another amplifier. According to radiation tests performed by the Jet Propulsion Laboratory (JPL), the amplification of the first type of amplifier is expected to drop by a factor of 3.2 for a dose between 50 and 500 krad, whereas that of the second one even increases up to 300 krad and drops only beyond 600 krad (JPL Galileo document 85-43). This is consistent with our observations that the response to the test pulses changed only in the IA, CA and EA channels: the amplifier for this channel is less radiation hard.

The relatively larger shifts in the test pulses in AR3 compared to those in the other channels can be understood by a shorter test pulse generated in this channel. The test pulses have a rectangular shape and due to the electronics degradation the operational amplifier becomes too slow to fully measure the entire test pulse.

In principle, shifts in the signals measured during test pulses might also be due to degradation of the test pulse generator. However, this can be excluded for the following reasons: The response changed only in the channels IA, EA and CA while the PA channel remained unchanged. If the test pulse generator had degraded, the response in PA should also have changed because all four channels were connected to the same test pulse generator. Furthermore, shifts in the rise times similar to those seen in the test pulses were also measured for the jovian dust stream particles which are real dust impacts (see below). Finally, the test pulse generator was a very simple device mostly consisting of resistors and did not contain any operational amplifiers so that it was less likely to suffer radiation damage. To summarise, the analysis of the charge amplitudes from the test pulses has shown that the sensitivity of the instrument for dust detection has degraded with time.

Shifts in the rise times were also seen in the signals measured during impacts of jovian dust stream particles. The averaged rise times gradually shifted from about 50 to 90 μs between 1996 and 2000 and stayed at that maximum value imposed by the electronics afterwards. Using the stream particles as "test particles" and assuming that their intrinsic characteristics did not change with time, this independently implies that the response of the instrument to dust impacts has changed.

Electronics degradation is also indicated by a gradual reduction of the charge amplitudes, IA and EA, measured for the jovian stream particles during the Jupiter mission.

The shifts in the signal rise times and charge amplitudes affect the mass and speed calibration and the identification of noise events in the dust data. This will be analysed in Section 4.

3.2. Channeltron amplification

Another indication for aging of the Galileo dust instrument electronics is displayed by a drop of the channeltron amplification. The amplification is expressed by the ratio between the charge amplitude measured during dust impacts at the channeltron and that measured on the ion collector grid, Q_C/Q_I or CA − IA if expressed in digital units. This ratio remained constant in interplanetary space (Grün et al., 1995a; Krüger et al., 1999a) but dropped continuously beginning with Galileo's Jupiter mission in 1996 (Krüger et al., 2001).

To compensate for the channeltron degradation, the channeltron voltage (HV) was increased a few times after mid-1999 (Table 2). This raised the Q_C/Q_I ratio close to its original value again. It should be noted that a reduction of the amplification with time is a normal aging effect seen in channeltrons. Thus, it is likely that the drop of the channeltron amplification was not solely caused by radiation damage.

3.3. Noise sensitivity

During Galileo's interplanetary cruise the lowest amplitude range (AR1) in classes 0 and 1 was contaminated with noise events whereas class 2 was free of noise (Baguhl et al., 1993). Later, within Jupiter's magnetosphere, class 2 was also strongly affected by noise (Krüger et al., 1999b). In order to analyse the instrumental response to noise events in these classes as a function of time, one has to identify time intervals when little or no dust impacts occurred. Jovian stream particles where measured throughout the jovian magnetosphere (Grün et al., 1998; Krüger et al., 2004). Due to the detection geometry, however, between 1996 and mid-2000 the dust instrument could detect these streams only within about 50 R_J from Jupiter. Further away, the streams were not in the field of view of the instrument. Hence, assuming that the background from other sources—in particular dust from interplanetary space—was negligible, data from these periods could be used to analyse the noise sensitivity of the instrument.

Fig. 4 shows the rates of class 0 and class 2 events during time periods around apojove (i.e. between 50 and 150 R_J) when no dust stream particles were detected (averages of typically 10–30 days). Within four years, both event rates dropped by about one (class 2) and two orders of magnitude (class 0), respectively. After mid-2000 the dust streams were detected during almost the entire Galileo orbit about Jupiter with a low impact rate. Thus, for 2002 we show the total count rate (dust stream impacts plus noise) which represents an upper limit for the noise rate. Fig. 4 clearly shows that the sensitivity for noise events has continuously dropped during Galileo's orbital mission.

Table 2
Channeltron high voltage digital settings (HV) of the Galileo dust instrument and corresponding voltages

Year-day	HV (dn)	Voltage (V)
Before 1999-305	2	~1020
1999-305	3	~1135
1999-345	4	~1250
2000-209	5	~1365
2001-352	6	~1480

One digital (dn) step corresponds to an amplification step of about a factor of 2. See Grün et al. (1995b) for further details of the channeltron settings.

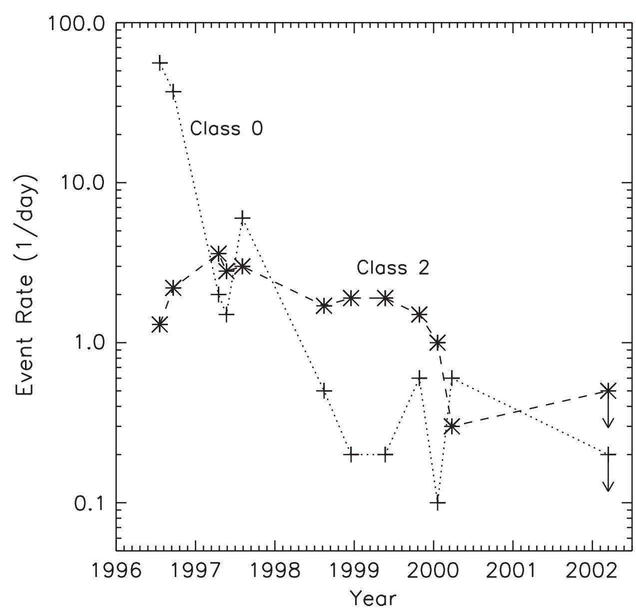

Fig. 4. Galileo event rate in class 0 (crosses) and class 2 (asterisks) during times when no dust stream particles could be detected (only amplitude range AR1). Mean values for time periods of 10–30 days are shown. For comparison: the typical class 0 event rate during interplanetary cruise (June 1994) was about 10 per day. After mid-2000 the dust stream particles were detected during almost Galileo's entire orbit so that there were no sufficiently long time intervals anymore during which the noise rate could be studied. Hence, in 2002 only an upper limit for noise plus dust impacts can be shown (indicated by arrows).

3.4. Threshold for dust impact detection

The analysis of the test pulses in Section 3.1 showed that the charge amplification and, hence, the sensitivity for dust impact detection decreased with time. The amplification dropped by a factor of 4.5 between 1996 and early-2002 (Fig. 3). As the instrumental threshold settings for charge detection in the target and iongrid channels remained unchanged, this also implies that the minimum impact charge detectable with the instrument increased by the same factor.

The reduction of the measured impact charges can be empirically described by linear relations:

$$Q_{\mathrm{I,true}} = Q_{\mathrm{I,meas}} \quad f_{\mathrm{I,corr}}, \tag{2}$$

$$Q_{\mathrm{E,true}} = Q_{\mathrm{E,meas}} \quad f_{\mathrm{E,corr}}. \tag{3}$$

$Q_{\mathrm{I,true}}$ and $Q_{\mathrm{E,true}}$ are the true impact charges generated by a dust impact. $Q_{\mathrm{I,meas}}$ and $Q_{\mathrm{E,meas}}$ are the charges measured by the (degraded) instrument electronics. The charge corrections, $f_{\mathrm{I,corr}}$ and $f_{\mathrm{E,corr}}$ ($f_{\mathrm{I,corr}} \geqslant 1$ and $f_{\mathrm{E,corr}} \geqslant 1$), can be determined from the test pulses independently for Q_{I} and Q_{E}. The charge signal measured at the channeltron, Q_{C}, is not considered because it strongly depends on the channeltron amplification and hence the channeltron voltage setting. It is therefore not used for mass calibration of dust impacts. In this section we use the charges in Coulomb rather than the digital units to quantify the drop of the instrument sensitivity.

The charges $Q_{\mathrm{I,meas}}$ and $Q_{\mathrm{E,meas}}$ measured during the test pulses are shown in Fig. 3. Linear fits to the data for the period after 1997 give the following correction factors:

$$f_{\mathrm{I,corr}} = (1 - 0.1335t)^{-1}, \tag{4}$$

$$f_{\mathrm{E,corr}} = (1 - 0.0916t)^{-1}. \tag{5}$$

The time t is measured in years since 1997.0. The charge correction expressed by Eqs. (2) and (3) has to be applied to the dust data beginning in 1997 until early 2002. No correction is necessary for earlier data. After January 2002 Galileo had two very long orbits until the mission ended in September 2003, including a close encounter with Jupiter in November 2002 (Fig. 2). Thus, one expects a rather constant instrument performance during the long orbits, interrupted by a strong drop in sensitivity during the close encounter. This is supported by the data: during Galileo's final passage through the inner jovian system in November 2002 the test pulses indicate another drop of the amplification by at least a factor of 1.5. Therefore Eq. (2) leads to an overestimation of the degradation and two constant values for the detection threshold for 2002 and 2003 are a better approximation (see Fig. 3).

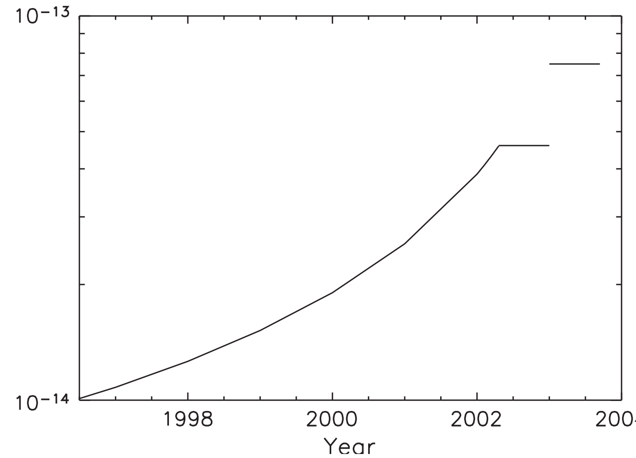

Fig. 5. Charge detection threshold Q_{I} (Coulomb) of the Galileo dust instrument as a function of time beginning in 1996. Before 1996 the detection threshold remained constant at 10^{-14} C.

The charge signal measured on the ion collector, Q_{I}, is used to trigger a measurement cycle of the instrument after a dust particle hit the detector target (Krüger et al., 2001, Q_{E} is not used because of high noise sensitivity of this channel). Hence, Eq. (2) describes the drop in the detection threshold for dust impacts. The initial detection threshold in 1996 was 10^{-14} C (Grün et al., 1995a) and the curve as a function of time is shown in Fig. 5. Due to the drop of the instrument sensitivity the later the measurements were performed, the bigger (or faster or both) the particles had to be in order to be detectable. The reduction in sensitivity was negligible during the early Jupiter mission of Galileo but became significant after 2000.

An indirect indication for a drop in the instrument sensitivity for dust detection came from the jovian stream particles: from 1996 to 2002 we have recognised a steady reduction by about two orders of magnitude in the average impact rate. Although the dust ejection of Io probably varied by orders of magnitude on timescales of weeks to months (Krüger et al., 2003a), and its long-term evolution is not known, this indicates that the instrument sensitivity had degraded.

4. Countermeasures for dust instrument aging

The analysis in Section 3 has demonstrated that the electronics of the Galileo dust instrument has degraded since the spacecraft began its orbital mission about Jupiter in December 1995. In particular, the instrument sensitivity as well as the speed and mass calibration for dust impacts have changed. In order to provide a dust data set from the entire Galileo mission as homogeneous as possible, instrument operation and data processing had to take these effects into account.

4.1. Instrument operation

Class 3 signals were always free of noise (with the possible exception of some very rare events in the inner jovian system, Krüger et al., 1999b) whereas all lower quality classes contain noise events. The noise identification technique developed for the jovian environment which is presented in Section 4.2 required a reliable subset of noise-free (class 3) dust impacts which could be used as a template for noise identification in the lower quality classes. Therefore, it was essential to always have class 3 impacts in the dust data. As the drop of the channeltron amplification (Section 3.2) gradually reduced the fraction of class 3 impacts in the data set, the channeltron voltage had to be raised a few times during the Jupiter mission (Table 2). This kept the fraction of class 3 impacts close to its original value.

4.2. Class 2 noise identification

In an earlier analysis (Krüger et al., 1999b) a set of parameters measured by the dust instrument was used to identify noise in the class 2 data and to separate the noise events from true dust impacts. Two important parameters for this scheme were the rise times of the charge signals on the target and on the ion collector grid, ET and IT, respectively. Rise time values caused by noise events differed from those of true dust impacts: noise events showed either very long or very short signal rise times. In addition, the difference between the charge amplitude at the target and that at the ion collector grid, $EA - IA$, had to fulfill certain constraints: in laboratory experiments the target signal for dust impacts was typically 2 to 6 digits larger than the ion charge signal ($2 \leqslant (EA - IA) \leqslant 6$). Only a fraction of the ions generated at the target reached the ion collector while the remaining ions were lost through the sensor opening or collected by the channeltron (Fig. 1). Hence, events outside this range in $EA - IA$ were classified as noise. Finally, for dust impacts the flight time between the target and the iongrid of ions generated during a dust impact, EIT, had to be in a physically plausible range. Either negative flight times (i.e. the ion grid signal occured before the target signal) or very long flight times were physically excluded and had to be due to noise events. Hence, the flight time between the target and the iongrid has to fulfill $4 \leqslant EIT \leqslant 13$ for dust impacts. Additional constraints used the entrance grid signal, PA, and the flight time between the entrance grid and the target, PET. These were purely empirical constraints because the entrance grid measurement of the dust instrument did so far not yield any meaningful results for dust impacts. For noise identification, however, it could be used as an additional parameter. For more details of the initial noise identification scheme for the Jupiter mission see Krüger et al. (1999b).

The electronics degradation revealed in Section 3 required a modified noise identification scheme for the later Galileo mission which is given in Table 3. Note that especially the constraints for the signal rise times were

Table 3
Time-dependent scheme to separate class 2 noise events from true dust impacts in the jovian system, taking into account degradation of the dust instrument electronics

Year	Orbits	AR1					
		Entrance grid amplitude PA	Target ampl. minus ion grid ampl. EA – IA	Rise time of target amplitude ET	Rise time of ion grid amplitude IT	Flighttime target-iongrid EIT	Flighttime entrance grid-target PET
1996	G1-E4	⩾8	⩽1 or ⩾7	⩽9 or ⩾14	⩽8	⩽3 or ⩾14	⩾1 and ⩽30
1997	J5-E12	⩾8	⩽1 or ⩾7	⩽9 or ⩾14	⩽9	⩽3 or ⩾14	⩾1 and ⩽30
1998	J13-E18	⩾8	⩽1 or ⩾7	⩽11 or ⩾15	⩽11	⩽3 or ⩾14	⩾1 and ⩽28
1999	E19-C21	⩾10	⩽1 or ⩾8	⩽12	⩽12	⩽6 or ⩾15	⩾2 and ⩽27
1999–2001	C22-I31	⩾10 and ⩽29	⩽1 or ⩾8	⩽13	⩽13	⩽6 or ⩾15	⩾2 and ⩽26
2001–2003	I32-A34	⩾10 and ⩽29	⩽1 or ⩾9	⩽13	⩽13	⩽6 or ⩾15	⩾2 and ⩽26

Year	Orbits	AR2 – AR6	
		Target amplitude minus ion grid amplitude EA – IA	Channeltron amplitude CA
1996–2003	G1-A34	⩽1 or ⩾7	⩽2

Noise events in the lowest amplitude range (AR1) fulfill at least one of the criteria listed above, whereas noise events in the higher amplitude ranges fulfill *all* criteria listed for AR2 – AR6 (see Grün et al., 1995b, for a definition of the parameters) The criteria for 1996 are those published by Krüger et al. (1999b). Each Galileo orbit had a targeted flyby at one moon which is identified by a letter in front of the orbit number. For example, "G28" was the 28th orbit, during which Galileo passed closest to Ganymede.

changed because the electronics degradation gradually increased the rise times measured for dust impacts. For dust impacts, the shift in the rise times also affected the measured flight time, leading to on average longer flight times between the target and the ion grid. The noise constraint for $EA-IA$ also had to be modified because the electronics aging lead to a faster degradation in IA than in EA (Fig. 3). Hence, for dust impacts, the constraint for $EA-IA$ had to be extended towards larger values. All class 2 events which fulfill the criteria listed in Table 3 are classified as noise events. All other class 2 events are considered true dust impacts.

All these considerations apply to AR1 only. In the higher amplitude ranges, AR2–AR6, simpler noise criteria based solely on the charge amplitudes were sufficient. In particular, no time-dependent scheme was required because EA and IA degraded by the same amount and the criteria published earlier remain valid for the entire mission.

With the noise criteria listed in Table 3 a homogeneous data set of class 3 and denoised class 2 dust impacts was obtained for the entire Galileo Jupiter mission. It contains the complete information (impact charges, signal rise times, impact direction etc.) of 18340 dust impacts and supplements the data set for 1996/97 published earlier (Krüger et al., 1999b, 2001). This time-dependent noise identification scheme was also applied to class 0 and class 1, but without success. The classification of class 0 and class 1 events as noise throughout the jovian magnetosphere remains valid in general, although the class 1 data from the short periods of Galileo's gossamer ring passages in November 2002 and September 2003 probably also contain true dust impacts. The analysis of the gossamer ring data is ongoing (Moissl, 2005).

4.3. Flux calculation for jovian dust stream particles

Due to the decrease of the dust detection threshold revealed in Section 3.4 a comparison of flux measurements from the late Galileo mission with earlier data can only be accomplished after an appropriate correction for the electronics degradation. However, the *flux* correction—for a given change in the detection threshold—depends on the grain size distribution: the steeper the slope of the size distribution the bigger the change in the number of detected grains. To derive fluxes of jovian dust stream particles for the entire Galileo Jupiter mission we assume that the intrinsic grain size distribution has not changed with time and that the measured *impact charge* distribution reflects the *size* distribution. Taking the charge distribution measured in 1996 (Fig. 6) as the intrinsic distribution before electronics degradation became significant, the expected drop in the dust flux is the number of particles above a given impact charge value relative to the number of all grains above

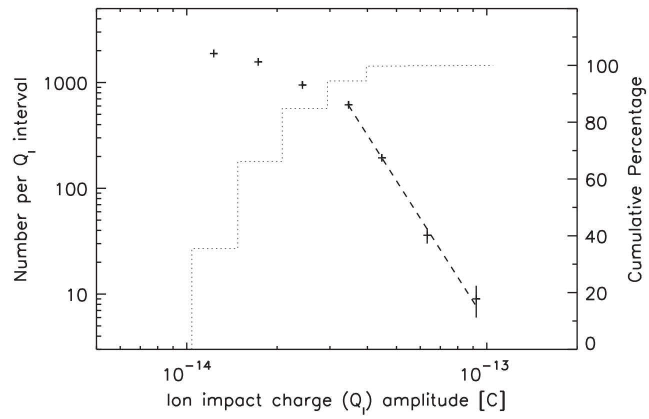

Fig. 6. Amplitude distribution of the impact charge Q_I for the dust particles detected in AR1 in 1996. The crosses indicate the number of impacts per charge interval, whereas the dotted line shows the cumulative distribution. Vertical bars indicate the $\sqrt{n}$ statistical fluctuation. A power law fit to the data with $3\times 10^{-14}\,C<Q_I<10^{-13}\,C$ is shown as a dashed line (power law index −4.46). From Krüger et al. (2001).

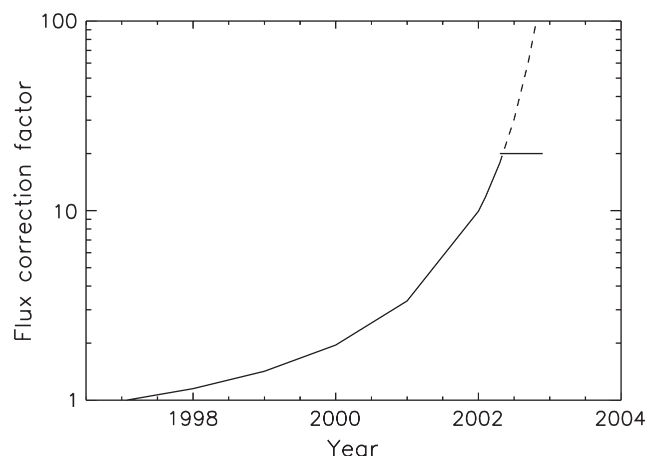

Fig. 7. Flux correction factor for jovian dust stream particles as a function of time. The dashed line is an extrapolation of the curve for 1996 to 2001 while the horizontal line represents a more realistic value for 2002.

the initial detection threshold (10^{-14} C). With the known charge distribution and the shift in the detection threshold with time given by Eq. (2) the drop in the measured flux can be expressed as a function of time. The resulting flux correction factor is

$$f_{\mathrm{flux}} = 10^{(-0.391+1/(2.5839-0.3728t))} \tag{6}$$

with the time t measured in years since 1997.0. f_{flux} is shown in Fig. 7. Dust stream fluxes measured at a given time have to be multiplied by f_{flux} in order to correct for electronics degradation.

The flux correction according to Eq. (6) is a factor of 20 in early-2002. For measurements later in 2002 this same factor should be used: because of the long Galileo orbits in 2002/03 the spacecraft spent long periods far away from the inner magnetosphere so that no further degradation occurred. Hence, Eq. (6) leads to an overestimation of the flux correction (see Section 3.4) and a constant value is a better approximation. Only very few data have been received after Galileo's last passage through the inner jovian magnetosphere in November 2002 so that the degradation and hence the flux correction are rather uncertain. A flux correction factor of at least a factor of 100 is indicated by the test pulses. Such a strong flux correction is also supported by the dust stream measurements: very few particles (and noise events) were measured during the final Galileo orbit in 2003, confirming that the instrument degradation was indeed very serious.

4.4. Speed and mass calibration

Two important parameters derived from the Galileo in-situ dust measurements are the impact speed and mass of the dust grains. The speed is derived from the charge rise times t_E and t_I, and the mass of a dust particle can only be derived from the charge amplitudes Q_E and Q_I once its impact speed is known (Eq. (1)).

A simple test for the applicability of the speed calibration late in the Galileo mission is provided by the dust data measured during the gossamer ring passage in November 2002: assuming that gossamer ring particles orbit Jupiter on circular Keplerian orbits, the expected impact speed is about $18\,\mathrm{km\,s^{-1}}$, and would be somewhat higher for eccentric orbits. About 90% of the dust impacts showed abnormally long signal rise times which led to extremely low calibrated impact speeds of only about $3\,\mathrm{km\,s^{-1}}$. Given that the typical error of the speed calibration obtained in the laboratory is a factor of two, this discrepancy implies severe shifts in the speed calibration. This was expected from the analysis of the test pulses. Masses derived for these abnormally low speeds are too large by up to 4 orders of magnitude. On the other hand, the speed measurements were very reliable during the early Jupiter mission: during close flybys at the Galilean moons the measured speeds agreed remarkably well with the flyby speed at these moons (Krüger et al., 2000, 2003c), showing that the detected grains were in steady-state dust clouds surrounding the moons. This confirmed the applicability of the speed calibration for the non-degraded electronics.

If the impact speed of the grains is known independently of the instrument calibration, the calculation of grain masses is rather straightforward, even with the degraded electronics: the measured impact charges can be corrected with Eqs. (2) and (3) and the Q/m calibration curves published by Grün et al. (1995a) give the—speed-dependent—conversion from impact charge to mass. This technique was successfully applied by Krüger et al. (2000, 2003c) to particles in the dust clouds surrounding the Galilean moons, even though no degradation correction was necessary at the time.

On the other hand, a correction for the impact speed calibration cannot simply be obtained with a shift in the measured rise times. The rise time is measured from a simple peak detection and the electronics starts measuring when the charge signal exceeds a given threshold. The signal peak is defined by drop of a certain amount after the signal has reached its maximum value. The electronics degradation led to reduced charge amplitudes and, hence, to extended rise times. This extension derived for rise times of about 30–40 μs from the test pulses cannot simply be extrapolated to the entire range of possible rise times between 10 and 100 μs because the actual pulse shape is not known and varies from impact to impact. Furthermore, the test pulse has a rectangular shape which is of course not the case for the signal from a true dust impact. The situation is further complicated because the digitisation of the analogue rise times is neither on a linear nor on a logarithmic scale (Grün et al., 1995a). Our analysis showed that a physically meaningful correction of the rise time measurement could not be derived. On the other hand, one may argue that the flight time of the grains between the entrance grid and the target, PET, can be used for a speed measurement. The charge measurements from the entrance grid, however, did not yield any meaningful results and therefore have to be discarded.

Hence, to calibrate masses for dust particles with unknown impact speed one has to rely on the instrument calibration as much as possible. As the shifts in rise time and charge amplitude were relatively small before 2000, speeds and masses have to be taken from the laboratory calibration (Grün et al., 1995a). Given the uncertainty of a factor of two in the speed and that of a factor of ten in the mass, the increased uncertainty due to the electronics degradation is relatively small. After 2000, the mass and speed calibration should be taken with caution because the degradation of the Galileo instrument was very severe. Only in cases where impact speeds are known from other arguments can corrected masses of particles be derived (e.g. the dust cloud measurements in the vicinity of the Galilean moons or Galileo's gossamer ring passages). It should be noted, however, that the speed and mass calibration obtained in the laboratory cannot be applied to the jovian stream particles anyway because these grains are beyond the calibrated range of the dust instrument (Zook et al., 1996). The calibration can only be applied to larger and slower particles.

5. Long-term dust studies at Jupiter

After noise removal (Section 4.2) and correcting for instrument degradation (Section 4.3) the Galileo data set

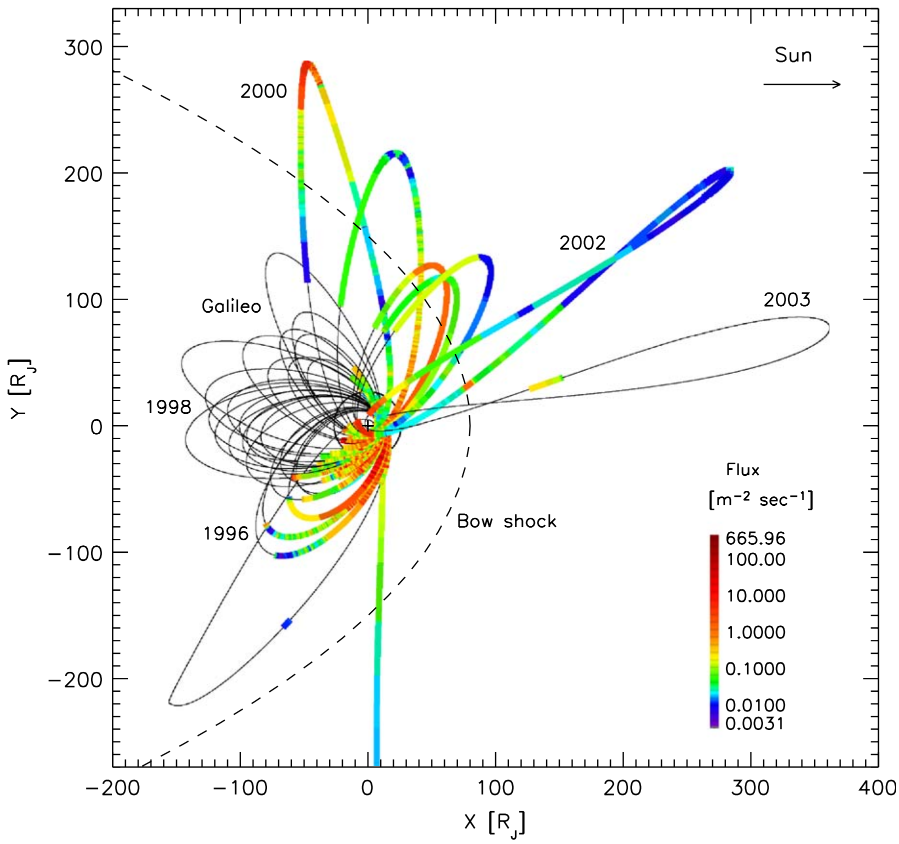

Fig. 8. Galileo's trajectory from 1996 to 2003 projected onto Jupiter's equatorial plane. The fluxes of jovian dust stream particles are superimposed in a colour scale (amplitude range AR1). For calculating the impact direction of the particles, a typical trajectory of a 10 nm particle was assumed (Grün et al., 1998). The flux has been corrected for electronics degradation according to Fig. 7. The rough location of the bow shock is indicated by a dashed parabola. The solid circle indicates Callisto's orbit and the Sun is to the right.

can be used for long-term dust studies in the jovian environment. An example is shown in Fig. 8 which shows fluxes of jovian dust stream particles superimposed upon the Galileo trajectory in the jovian system. The time-variable detection area of the sensor has been calculated with a "typical" trajectory of a 10 nm dust particle (Grün et al., 1998). In regions where no flux is shown, the dust streams were either not detectable, because the dust detector was pointing in the wrong direction (most of the time when no flux is shown), or no dust data were transmitted to Earth. Each Galileo orbit had a targeted flyby at one moon which is identified by a letter in front of the orbit number. For example, "G28" was the 28th orbit, during which Galileo passed closest to Ganymede. Several features are obvious in Fig. 8:

(1) Fluxes of dust stream particles were highly variable by about five orders of magnitude, between 3×10^{-3} and $6 \times 10^{2}\,\mathrm{m^{-2}\,s^{-1}}$. The corresponding number density of dust stream particles in the jovian environment varied from 10^{-8} to $10^{-3}\,\mathrm{m^{-3}}$.

(2) The dust flux was usually higher close to Jupiter, as one would expect if the dust source is located in the inner jovian system. The radial dependence of the flux showed strong variations from orbit to orbit. Only in early 2001 (G29 orbit), was a nearly perfect r^{-2} drop measured, as one expects from simple particle dispersion in space. Taking all orbits since 1996 together, slopes between -1 and -5 were found. These variations could be due to fluctuations in Io's dust production or the plasma conditions in the Io torus and the jovian magnetosphere or both.

(3) In 2000 (G28 orbit), the dust flux measured by Galileo was about three orders of magnitude larger outside the magnetosphere ($\sim 10\,\mathrm{m^{-2}\,s^{-1}}$; radial distance from Jupiter about $280\,R_\mathrm{J}$) than within the magnetosphere (Krüger and Grün, 2002). Such a high flux was only rarely measured in this spatial region. A rather high flux ($\sim 1\,\mathrm{m^{-2}\,s^{-1}}$) occurred again in mid-2001 (C30 orbit), whereas other orbits showed a low dust flux at comparable spatial locations (G29, I31, I32, I33; $0.1 \ldots 0.01\,\mathrm{m^{-2}\,s^{-1}}$). The three orders of magnitude increase in dust emission in G28 is coincident with a factor of three increase in the neutral gas production of Io in the same time period (Delamere et al., 2004).

(4) The Galileo long-term record of jovian dust stream measurements revealed a large orbit-to-orbit variation due to both systematic and stochastic changes.

Systematic effects include Io's orbital motion, changes in the geometry of Galileo's orbit and in the magnetic field configuration due to the rotation of the planet. Stochastic variations include fluctuations of Io's volcanic activity and the deformation of the outer magnetosphere in response to the variable solar wind conditions. Using the long record of Galileo's dust measurements, the variability due to stochastic variations could be approximately removed by "averaging" and a strong variation with jovian local time showed up (Krüger et al., 2003b). This result confirmed theoretical expectations (Horányi et al., 1997), predicting higher dust fluxes on the dawn and dusk sides of Jupiter's magnetosphere than at noon. The dust fluxes are sensitive to the spatially varying plasma conditions in the Io plasma torus, and the grains provide a "tomography" of the Io torus.

One additional facet of the Galileo dust streams measurements since 1996 is that they can act as a monitor of Io's volcanic activity (Krüger et al., 2003a). As a dust source, Io can be considered as a minor source of interplanetary dust. About $10\,\mathrm{g\,s^{-1}}$ to $10\,\mathrm{kg\,s^{-1}}$ of dust are continuously released from Io, consistent with theoretical predictions (Ip, 1996). This is less than 1% of the total plasma mass ejected from Io into the torus. Io is also a minor dust source compared to the dust generated from comets or main belt asteroids ($\sim 10^4\,\mathrm{kg\,s^{-1}}$).

The dust data set derived in this paper has been used for several investigations of jovian dust published already, including various time-variable phenomena (Krüger et al., 2004, and references therein). These earlier publications have used the corrected data set and, hence, their results remain unchanged. The dust data set is available via the Planetary Data System and the Heidelberg Dust Group (http://www.mpi-hd.mpg.de/dustgroup/galileo). The data set will be the basis for further investigations of jovian dust in the future like, e.g., the dust measurements from Galileo's gossamer ring passages in November 2002 and September 2003 which is ongoing.

A twin of the Galileo dust instrument has been operational on the Ulysses spacecraft in interplanetary space since 1990 and a flight-spare unit of the detector (Gorid) measured dust in geostationary orbit on board the Express 2 satellite between 1997 and 2002 (Drolshagen et al., 1999). So far, the Ulysses detector does not show significant degradation, consistent with its exposure to a much lower radiation dose compared to the Galileo instrument. Since 2004 the Cassini spacecraft which is equipped with an upgrade of the Galileo and Ulysses dust instruments (Srama et al., 2004) has been exploring the saturnian system. The experience gained from the Galileo instrument operation at Jupiter will be useful for future studies of interplanetary and circumplanetary dust phenomena with all four instruments.

Acknowledgements

The authors wish to thank the Galileo project at NASA/JPL for effective and successful mission operations. This research has been supported by the German Bundesministerium für Bildung und Forschung through Deutsches Zentrum für Luft- und Raumfahrt e. V. (DLR, grant 50 QJ 9503 3). Support by Max-Planck-Institut für Kernphysik (MPIK) is also gratefully acknowledged. We thank two anonymous referees for very useful comments improving the presentation of our results.

References

Auer, S., 2001. In: E. Grün, B.A.S. Gustafson, S.F. Dermott, H. Fechtig (Eds.), Interplanetary Dust, Springer, Berlin, Heidelberg, New York, pp 385–444.

Baguhl, M., 1993. Identifikation von Staubeinschlägen in den Daten der Mikrometeoriden-Detektoren an Bord der Raumsonden Ulysses und Galileo, Ph.D. Thesis, Ruprecht-Karls-Universität, Heidelberg.

Baguhl, M., Grün, E., Linkert, G., Linkert, D., Siddique, N., 1993. Identification of 'small' dust impacts in the Ulysses dust detector data. Planetary and Space Science 41, 1085–1098.

Colwell, J.E., Horányi, M., Grün, E., 1998a. Jupiter's exogenic dust ring. Journal of Geophysical Research 103, 20023–20030.

Colwell, J.E., Horányi, M., Grün, E., 1998b. Capture of interplanetary and interstellar dust by the Jovian magnetosphere. Science 280, 88–91.

Delamere, P.A., Steffl, A., Bagenal, F., 2004. Modeling temporal variability of plasma conditions in the Io torus during the Cassini era. Journal of Geophysical Research-Space Physics 109 (A18), 10216.

Drolshagen, G., Svedhem, H., Grün, E., Grafodatsky, O., Prokopiev, U., 1999. Microparticles in the geostationary orbit (GORID experiment). Advances in Space Research 23, 123–133.

Göller, J.R., Grün, E., 1985. In: Giese, R.H., Lamy, P. (Eds.), Properties and Interaction of Interplanetary Dust, Reidel, Dordrecht, pp. 113–115.

Graps, A.L., Grün, E., Svedhem, H., Krüger, H., Horányi, M., Heck, A., Lammers, S., 2000. Io as a source of the Jovian dust streams. Nature 405, 48–50.

Grün, E., Fechtig, H., Hanner, M.S., Kissel, J., Lindblad, B.A., Linkert, D., Maas, D., Morfill, G.E., Zook, H.A., 1992. The Galileo dust detector. Space Science Reviews 60, 317–340.

Grün, E., Baguhl, M., Hamilton, D.P., Kissel, J., Linkert, D., Linkert, G., Riemann, R., 1995a. Reduction of Galileo and Ulysses dust data. Planetary and Space Science 43, 941–951.

Grün, E., Baguhl, M., Divine, N., Fechtig, H., Hamilton, D.P., Hanner, M.S., Kissel, J., Lindblad, B.A., Linkert, D., Linkert, G., Mann, I., McDonnell, J.A.M., Morfill, G.E., Polanskey, C., Riemann, R., Schwehm, G.H., Siddique, N., Staubach, P., Zook, H.A., 1995b. Three years of Galileo dust data. Planetary and Space Science 43, 953–969.

Grün, E., Krüger, H., Graps, A., Hamilton, D.P., Heck, A., Linkert, G., Zook, H., Dermott, S.F., Fechtig, H., Gustafson, B., Hanner, M., Horányi, M., Kissel, J., Lindblad, B., Linkert, G., Mann, I., McDonnell, J.A.M., Morfill, G.E., Polanskey, C., Schwehm, G.H., Srama, R., 1998. Galileo observes electromagnetically coupled dust in the Jovian magnetosphere. Journal of Geophysical Research 103, 20011–20022.

Grün, E., Krüger, H., Landgraf, M., 2001. In: Balogh, A., Marsden, R., Smith, E. (Eds.), The Heliosphere at Solar Minimum: The Ulysses Perspective, Springer Praxis, pp. 373-404.

Horányi, M., Grün, E., Heck, A., 1997. Modeling the Galileo dust measurements at Jupiter. Geophysical Research Letters 24, 2175–2178.

Ip, W.H., 1996. The dust halo of Io. Geophysical Research Letters 24, 3671–3674.

Krivov, A.V., Krüger, H., Grün, E., Thiessenhusen, K.-U., Hamilton, D.P., 2002a. A tenuous dust ring of Jupiter formed by escaping ejecta from the Galilean satellites. Journal of Geophysical Research 107, E1.

Krivov, A.V., Wardinski, I., Spahn, F., Krüger, H., Grün, E., 2002b. Dust on the outskirts of the Jovian system. Icarus 157, 436–455.

Krüger, H., 2003. Jupiter's Dust Disc, An Astrophysical Laboratory, Shaker Verlag Aachen, ISBN 3-8322-2224-3, Habilitation Thesis Ruprecht-Karls-Universität Heidelberg.

Krüger, H., Grün, E., 2002. In: Green, S.F., Williams, I., McDonnell, T., McBride, N. (Eds.), Cospar Colloquia Series, vol. 15. Dust in the solar system and in other planetary systems. Pergamon Press, New York, pp. 144–159.

Krüger, H., Grün, E., Hamilton, D.P., Baguhl, M., Dermott, S.F., Fechtig, H., Gustafson, B.A., Hanner, M.S., Horányi, M., Kissel, J., Lindblad, B.A., Linkert, D., Linkert, G., Mann, I., McDonnell, J.A.M., Morfill, G.E., Polanskey, C., Riemann, R., Schwehm, G.H., Srama, R., Zook, H.A., 1999a. Three years of Galileo dust data: II. 1993 to 1995. Planetary and Space Science 47, 85–106.

Krüger, H., Grün, E., Heck, A., Lammers, S., 1999b. Analysis of the sensor characteristics of the Galileo dust detector with collimated Jovian dust stream particles. Planetary and Space Science 47, 1015–1028.

Krüger, H., Krivov, A.V., Hamilton, D.P., Grün, E., 1999c. Detection of an impact-generated dust cloud around Ganymede. Nature 399, 558–560.

Krüger, H., Krivov, A.V., Grün, E., 2000. A dust cloud of Ganymede maintained by hypervelocity impacts of interplanetary micrometeoroids. Planetary and Space Science 48, 1457–1471.

Krüger, H., Grün, E., Graps, A.L., Bindschadler, D.L., Dermott, S.F., Fechtig, H., Gustafson, B.A., Hamilton, D.P., Hanner, M.S., Horányi, M., Kissel, J., Lindblad, B., Linkert, D., Linkert, G., Mann, I., McDonnell, J.A.M., Morfill, G.E., Polanskey, C., Schwehm, G.H., Srama, R., Zook, H.A., 2001. One year of Galileo dust data from the jovian system: 1996. Planetary and Space Science 49, 1285–1301.

Krüger, H., Geissler, P., Horányi, M., Graps, A.L., Kempf, S., Srama, R., Moragas-Klostermeyer, G., Moissl, R., Johnson, T.V., Grün, E., 2003a. Jovian dust streams: A Monitor of Io's volcanic plume activity. Geophysical Research Letters 30, 2101–2105.

Krüger, H., Horányi, M., Grün, E., 2003b. Jovian dust streams: Probes of the Io plasma torus. Geophysical Research Letters 30, 1058–1061.

Krüger, H., Krivov, A.V., Sremčević, M., Grün, E., 2003c. Galileo measurements of impact-generated dust clouds surrounding the Galilean satellites. Icarus 164, 170–187.

Krüger, H., Horányi, M., Krivov, A.V., Graps, A.L., 2004. Jovian dust: streams, clouds and rings, Jupiter. The Planet, Satellites and Magnetosphere. In: Bagenal, F., Dowling, T.E., McKinnon, W.B. (Eds.), Cambridge Planetary Science, Vol. 1, Cambridge University Press, Cambridge, UK, ISBN 0-521-81808-7, 2004, pp. 219–240.

Moissl, R., 2005. Galileos Staubmessungen in Jupiters Gossamer-Ringen, Diplom thesis, University of Heidelberg.

Morfill, G.E., Grün, E., Johnson, T.V., 1980. Dust in Jupiter's magnetosphere—Physical processes. Planetary and Space Science 28, 1087–1100.

O'Neil, W.J., 1997. In: Barbieri, C., Rahe, J.H., Johnson, T.V., Sohus, A.M. (Eds.), Proceedings of The Three Galileos: The Man, The Spacecraft, The Telescope, Kluwer Academic Publishers, Dordrecht, pp. 17–32.

Srama, R., Ahrens, T.J., Altobelli, N., Auer, S., Bradley, J.G., Burton, M., Dikarev, V.V., Economou, T., Fechtig, H., Görlich, M., Grande, M., Graps, A.L., Grün, E., Havnes, O., Helfert, S., Horányi, M., Igenbergs, E., Jeßberger, E.K., Johnson, T.V., Kempf, S., Krivov, A.V., Krüger, H., Moragas-Klostermeyer, G., Lamy, P., Landgraf, M., Linkert, D., Linkert, G., Lura, F., Mocker-Ahlreep, A., McDonnell, J.A.M., Möhlmann, D., Morfill, G.E., Müller, M., Roy, M., Schäfer, G., Schlotzhauer, G.H., Schwehm, G.H., Spahn, F., Stübig, M., Svestka, J., Tschernjawski, V., Tuzzolino, A.J., Wäsch, R., Zook, H.A., 2004. The Cassini Cosmic Dust Analyzer. Space Science Reviews 114, 465–518.

Sremčević, M., Krivov, A.V., Krüger, H., Spahn, F., 2005. Impact-generated dust clouds around planetary satellites: model versus Galileo data. Planetary and Space Science 53, 625–641.

Thiessenhusen, K.-U., Krüger, H., Spahn, F., Grün, E., 2000. Dust grains around Jupiter—The observations of the Galileo Dust Detector. Icarus 144, 89–98.

Zook, H.A., Grün, E., Baguhl, M., Hamilton, D.P., Linkert, G., Linkert, D., Liou, J.-C., Forsyth, R., Phillips, J.L., 1996. Solar wind magnetic field bending of Jovian dust trajectories. Science 274, 1501–1503.